BIOCHEMICAL PHARMACOLOGY 75 (2008) 1393–1401

journal homepage: www.elsevier.com/locate/biochempharm

Cyanidin 3-glucoside protects 3T3-L1 adipocytes against H_2O_2- or TNF-α-induced insulin resistance by inhibiting c-Jun NH_2-terminal kinase activation

*Honghui Guo, Wenhua Ling *, Qing Wang, Chi Liu, Yan Hu, Min Xia*

Department of Nutrition, School of Public Health, Sun Yat-Sen University (Northern Campus), 74 Zhongshan Road 2, Guangzhou, Guangdong Province 510080, PR China

ARTICLE INFO

Article history:
Received 19 October 2007
Accepted 28 November 2007

Keywords:
Anthocyanin
Cyanidin 3-glucoside
c-Jun NH_2-terminal kinase
Insulin resistance
3T3-L1 adipocyte

ABSTRACT

Anthocyanins are naturally occurring plant pigments and exhibit an array of pharmacological properties. Our previous study showed that black rice pigment extract rich in anthocyanin prevents and ameliorates high-fructose-induced insulin resistance in rats. In present study, cyanidin 3-glucoside (Cy-3-G), a typical anthocyanin most abundant in black rice was used to examine its protective effect on insulin sensitivity in 3T3-L1 adipocytes exposed to H_2O_2 (generated by adding glucose oxidase to the medium) or tumor necrosis factor α (TNF-α). Twelve-hour exposure of 3T3-L1 adipocytes to H_2O_2 or TNF-α resulted in the increase of c-Jun NH_2-terminal kinase (JNK) activation and insulin receptor substrate 1 (IRS1) serine 307 phosphorylation, concomitantly with the decrease in insulin-stimulated IRS1 tyrosine phosphorylation and cellular glucose uptake. Blocking JNK expression using RNA interference efficiently prevented the H_2O_2- or TNF-α-induced defects in insulin action. Pretreatment of cells with Cy-3-G reduced the intracellular production of reactive oxygen species, the activation of JNK, and attenuated H_2O_2- or TNF-α-induced insulin resistance in a dose-dependent manner. In parallel, *N*-acetyl-cysteine, an antioxidant compound, did not exhibit an attenuation of TNF-α-induced insulin resistance. Taken together, these results indicated that Cy-3-G exerts a protective role against H_2O_2- or TNF-α-induced insulin resistance in 3T3-L1 adipocytes by inhibiting the JNK signal pathway.

1. Introduction

Insulin resistance, or an attenuated biological response to insulin, is a major pathological feature of diabetes and a central component in the so-called metabolic syndrome [1]. The exact mechanisms responsible for this abnormality are still not fully elucidated. Insulin physiologically initiates its biological function by activating the insulin receptor, resulting in tyrosine phosphorylation of insulin receptor substrate (IRS) proteins, such as IRS1 and IRS2. Tyrosine phosphorylation of IRS1 triggers downstream signaling pathways, and finally stimulates the translocation of glucose transporter 4 (GLUT4)

* *Corresponding author*. Tel.: +86 20 87331597; fax: +86 20 87330446.
E-mail address: lingwh@mail.sysu.edu.cn (W. Ling).

Abbreviations: 2-DG, 2-deoxy-D-glucose; Cy-3-G, cyanidin 3-glucoside; DCF-DA, dihydrodichlorofluorescein diacetate; DMEM, Dulbecco's modified Eagle's medium; FBS, fetal bovine serum; GLUT4, glucose transporter 4; IRS1, insulin receptor substrate 1; JNK, c-Jun NH_2-terminal kinase; KRP, Krebs-Ringer's phosphate; MTT, 3-(4,5-dimethylthiazol-2-yl)-2,5-diphenyl tetrazolium bromide; NAC, *N*-acetyl-cysteine; PM, plasma membrane; PY, phosphotyrosine; ROS, reactive oxygen species; siRNA, small interfering RNA; TNF-α, tumor necrosis factor α; TNFR1, TNF type-1 receptor; TRAF2, TNFR-associated factor 2.

0006-2952/$ – see front matter
doi:10.1016/j.bcp.2007.11.016

to facilitate the transport of glucose into cells [2,3]. Several extracellular agents and stress stimuli, such as free fatty acids, H_2O_2 and tumor necrosis factor α (TNF-α), all of which are known contributors to insulin resistance, induce phosphorylation of IRS1 at the inhibitory site serine 307 (Ser^{307}) [4–6]. Ser^{307} is located next to the phosphotyrosine-binding (PTB) domain in IRS1 and its phosphorylation inhibits the interaction of the PTB domain with the phosphorylated NPEY motif in the activated insulin receptor, thereby leading to inhibition of insulin signaling [7]. Although a variety of serine/threonine kinases have been described to be capable of mediating IRS1 phosphorylation [8], recent genetic evidence and emerging pharmacological data indicate that c-Jun NH_2-terminal kinase (JNK; also named stress-activated protein kinase, SAPK) may play a pivotal role in causing insulin resistance [9–11].

Recently, much attention has been paid to the physiological effects of some food components that may be beneficial in preventing insulin resistance and possibly reduce risks of diabetes and metabolic syndrome. Anthocyanins are naturally occurring polyphenolic compounds in the plant foods and widely distributed in fruits, vegetables, and pigmented cereals [12]. Many studies have shown that anthocyanin not only imparts color to plants but also exhibits an array of pharmacological properties, such as antioxidative, anti-inflammatory and antitumor activities [13]. Epidemiological investigations have indicated that the moderate consumption of anthocyanins through the intake of red wine is associated with a lower risk of coronary heart disease and metabolic syndrome [14,15]. In two recent reports, anthocyanins from purple corn and cherry have been shown to ameliorate obesity and insulin resistance in high-fat-fed mice [16,17]. Our previous study also demonstrated that black rice pigment extract rich in anthocyanin prevented and attenuated the insulin resistance induced by a high-fructose diet in animal model [18]. However, the molecular mechanism underlying this action remains unknown and needs further investigation in cells.

Considering the key role of JNK activation in the progression of insulin resistance and the potential capability of anthocyanin in preventing insulin resistance, we observed the influence of cyanidin 3-glucoside (Cy-3-G), a typical anthocyanin in black rice and other higher plants [13,19], on insulin resistance of 3T3-L1 adipocytes induced by exposure to H_2O_2 enzymatic-generating system or TNF-α. The signal pathway of the action involved in JNK molecular activation was also investigated.

2. Materials and methods

2.1. Cells and materials

Mouse embryo 3T3-L1 cells were obtained from China Center for Type Culture Collection (Wuhan, China). Dulbecco's modified Eagle's medium (DMEM), fetal bovine serum (FBS), and antibiotic mixture (penicillin-streptomycin) were purchased from the Gibco BRL (Grand Island, NY, USA). Anti-GLUT4, anti-IRS1, anti-p-$IRS1^{Ser307}$, anti-phosphotyrosine, anti-β-actin, and anti-JNK1 antibodies, and protein A/G plus agarose were obtained from Santa Cruz Biotech. (Santa Cruz, CA, USA). Anti-p-JNK (Thr183/Tyr185) antibody was obtained from Cell Signaling Technology (Danvers, MA, USA). Recombinant human TNF-α was purchased from CytoLab (Rehovot, Israel); short-acting human insulin, from Novo Nordisk (Bagsvaerd, Denmark); HPLC grade Cy-3-G, from Polyphenol AS (Sandnes, Norway); [1,2-^{3}H] 2-deoxy-D-glucose (^{3}H-2-DG), from GE Healthcare (Buckinghamshire, UK); and all other chemicals, unless otherwise specified, from Sigma (St. Louis, MO, USA).

2.2. Cell culture and treatments

3T3-L1 pre-adipocytes were grown to confluence in DMEM containing 10% FBS and 100 U/mL penicillin-streptomycin at 37 °C in a humidified atmosphere of 5% CO_2. Cells were induced to differentiate to adipocytes 24 h after confluence by changing the medium to DMEM supplemented with 10% FBS, 5 μg/mL insulin, 0.5 mM 3-isobutyl-methyl-xanthine and 0.25 mM dexamethasone sodium phosphate for 48 h. Thereafter, the cells were maintained in the original propagation DMEM, changing medium every 2 days until use. Unless indicated otherwise, cells were used 9–10 days after differentiation induction when exhibiting more than 90% adipocyte phenotype. H_2O_2 was generated by adding 50 mU/mL glucose oxidase to serum-free DMEM supplemented with 0.5% BSA. The addition of 50 mU/mL glucose oxidase resulted in medium H_2O_2 concentration that achieved a steady state of 11.3 ± 1.7 μM after 30 min, as previously reported [20]. Differentiated adipocytes were treated with various concentrations of anthocyanin Cy-3-G, antioxidant N-acetyl-cysteine (NAC), or JNK inhibitor SP600125 (Calbiochem, San Diego, CA, USA) before they were exposed to the H_2O_2 generating system or 1 nM TNF-α as indicated in each experiment.

2.3. Cytotoxicity tests

Cy-3-G and H_2O_2 induced cytotoxicity was measured using MTT dye [3-(4,5-dimethylthiazol-2-yl)-2,5-diphenyl tetrazolium bromide] as previously described [21]. The cells were seeded and differentiated in 24-well plates. After 12 h treatment with Cy-3-G (0, 10, 20, and 40 μM), or 50 mU/mL glucose oxidase, 0.5 mg/mL MTT was added to each well and incubated for 4 h to form formazan crystals. Then, the medium was gently removed and the crystals were dissolved in 1 mL of DMSO. Formazan crystals formed were quantified at 570 nm using an ELx800 reader (Bio-Tek Instruments Inc., Winooski, VT, USA). Cytotoxicity was expressed in terms of cell viability, as a ratio of the treatments to the PBS buffer control population.

2.4. Free radical scavenging activity assay

A fluorescent probe, dihydrodichlorofluorescein diacetate (DCF-DA), was used to measure intracellular reactive oxygen species (ROS) formation as described [22]. Briefly, cells were incubated with 10, 20, or 40 μM of Cy-3-G or 1 mM NAC for 12 h, before the 12-h exposure to H_2O_2 generating system or 1 nM TNF-α. Then, cells were washed twice in Krebs-Ringer's phosphate (KRP) buffer (130 mM NaCl, 5 mM KCl, 1.3 mM $CaCl_2$, 1.3 mM $MgSO_4$, 10 mM Na_2HPO_4, pH 7.4), incubated in pre-warmed KRP containing 5 mM glucose and 5 μM DCF-DA, and placed at 37 °C for 30 min. The reaction system was

washed three times with KRP. After centrifugation at 1000 × *g* for 5 min, the supernatants were removed and the pellets were resolved with 1% Triton X-100. Fluorescence was measured at an excitation wavelength of 480 nm and an emission wavelength of 525 nm using a Cary Eclipse fluorescence spectrophotometer (Varian, Palo Alto, CA, USA). Fluorescence values were calculated after subtracting background fluorescence levels, measured under identical conditions but without DCF-DA.

2.5. Glucose transport determination

The determination for glucose uptake was described previously with some modifications [4]. Serum-starved adipocytes were incubated with pre-warmed KRP containing 0.2% BSA and 10 nM insulin for 30 min. After this period, ^{3}H-2-DG and unlabeled 2-DG were dispensed into each well for a final concentration of 1 μCi/mL and 0.1 mM, respectively. Cells were incubated for an additional 10 min at 37 °C, and the reaction was terminated by three washes with ice-cold KRP. Cells were lysed in 100 μL 0.1 M NaOH, and radioactivity was determined by using a liquid scintillation counter (Canberra-Packard, Zellik, Belgium). Data were expressed as moles ^{3}H-2-DG per minute per milligram of lysate protein, which was determined using the bicinchoninic acid method. Nonspecific uptake was assessed in the presence of 10 μM cytochalasin B and subtracted from all of the measured values. Nonspecific uptake and absorption was always less than 8% of the total uptake.

2.6. JNK protein knockdown

To knockdown JNK1 protein expression, we performed transfection of mouse JNK1 small interfering RNA (siRNA) duplex with adipocytes on day 6 after differentiation. One microliters of INTERFERin transfection reagent (Polyplus transfection SA, Illkrich, France) was added to 200 μL of DMEM serum-free medium containing 6 nM of each siRNA oligo, incubated for 10 min, and added to the 12-well dishes containing 1 mL of fresh medium. A nonrelated, scrambled siRNA was used as a control. All siRNA oligos were designed and synthesized by Santa Cruz. Twenty-four, 48, and 72 h post-transfection, cells were lysed and subjected to SDS-PAGE and Western blot analysis to evaluate intracellular JNK1 protein levels.

2.7. Immunoprecipitation and Western blotting

Crude plasma membrane (PM) was prepared as described by Karlsson et al. with modifications [23]. Adipocytes were homogenized in 0.32 M sucrose, 5 mM Tris–HCl, 120 mM KCl, 1 mM EDTA, 0.5 mM EGTA, pH 7.5, with protease inhibitors (10 μM leupeptin, 1 μM pepstatin, 1 μM aprotinin, 4 mM iodoacetate, and 50 μM phenylmethylsulfonyl fluoride) using a Dounce glass homogenizer on slushy ice. A PM-containing pellet, obtained by centrifugation at 25,000 × *g* for 1.5 h at 4 °C, was resuspended in 20 mM HEPES, 1 mM EDTA, pH 7.4, with protease inhibitors, and was used for immunoblotting as described below.

To obtain total proteins, cells were lysised with a buffer containing 20 mM Tris–Cl, 150 mM NaCl, 1% Nonidet P-40, 0.5% sodium deoxycholate, 1 mM EDTA, 0.1% SDS, and protease inhibitors, pH 7.5. The lysates were centrifuged at 12,000 × *g* for 15 min, and the supernatants were used for immunoprecipitation and immunoblotting. For immunoprecipitation, the supernatants were incubated with antibodies against IRS1 overnight, then shook gently with the addition of protein A/G plus agarose for 2 h, centrifuged at 1000 × *g* for 5 min. Washed the pellet four times with 1 mL PBS, each time repeating the centrifugation step, collected and resuspended the immunoprecipitates pellet in 50 μL of electrophoresis sample buffer. Protein extractions were separated by using SDS-PAGE on 10% (for GLUT4 and JNK1) or 8% (for IRS1) polyacrylamide gels, and transferred to polyvinylidene difluoride (PVDF) membranes (Millipore, Billerica, MA, USA). After blocking for 2 h with 5% skimmed milk in TBS-T buffer (10 mM Tris, 150 mM NaCl, and 0.1% Tween-20), the membrane was incubated with primary antibodies against GLUT4, IRS1, p-IRS1^{Ser307}, phosphotyrosine (PY), β-actin, JNK1 and p-JNK for 2 h. Specific antibody binding was detected by horseradish peroxidase-conjugated secondary antibodies and visualized using enhanced chemiluminescence detection reagent (Santa Cruz). The band densities were quantified using an image analyzer Quantity One System (Bio-Rad, Richmond, CA, USA). All protein quantifications were adjusted for the corresponding β-actin level, which was not consistently changed by the different treatment conditions.

2.8. Statistical analysis

Statistical analyses were performed using the SPSS 11.0 package (SPSS Inc., Chicago, IL, USA). The results are presented as the mean ± S.E.M. of at least three-independent experiments. Data were analyzed by one-way ANOVA and a *post hoc* least significant difference (LSD)–*t* multiple comparisons test. The level of significance was set at $P < 0.05$.

3. Results

3.1. Cytotoxicity and radical scavenging activity of Cy-3-G

The results of the MTT assay showed that there was no significant change in cell viability after 12-h treatment with 40 μM Cy-3-G or 50 mU/mL glucose oxidase (data not shown).

Next, we measured ROS in adipocytes treated with 50 mU/mL glucose oxidase or 1 nM TNF-α. The DCF-DA probe could be oxidized to highly fluorescent compound dichlorofluorescein (DCF) by intracellular ROS or low-molecular weight peroxides. In adipocytes treated with 50 mU/mL glucose oxidase or 1 nM TNF-α for 12 h, the mean DCF fluorescence was increased 4.7-fold ($P < 0.01$) and 1.9-fold ($P < 0.05$), respectively, as compared to control cells (Fig. 1). However, this effect was almost abolished by pretreatment of 3T3-L1 adipocytes with 20 μM or 40 μM Cy-3-G, or 1 mM NAC for 12 h.

3.2. H_2O_2 and TNF-α inhibited the insulin-stimulated glucose uptake in 3T3-L1 adipocytes

It has been reported that H_2O_2 or TNF-α induces a defect of insulin signaling in 3T3-L1 adipocytes in a few hours to several days at different concentrations [20,22,24]. Thus, we

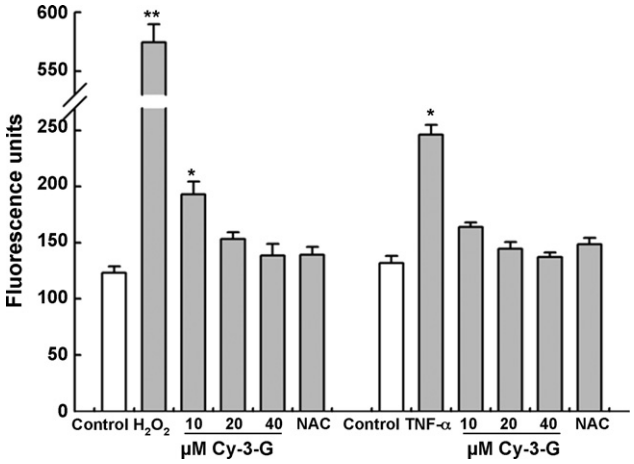

Fig. 1 – Cy-3-G and NAC decreased intracellular ROS levels in 3T3-L1 adipocytes treated with H_2O_2 or TNF-α. Fully differentiated 3T3-L1 adipocytes were pretreated for 12 h with 10, 20, or 40 μM of Cy-3-G, or 1 mM NAC, respectively, and subsequently incubated with ~12 μM H_2O_2 (generated by adding 50 mU/mL glucose oxidase to the medium) or 1 nM TNF-α for 12 h. Cell lysates were prepared, and intracellular ROS was measured using the fluorescent probe, DCF-DA. Results are the mean ± S.E.M. of triplicate determinations of four experiments and are expressed as fluorescence units detected in a fluorescence spectrophotometer. *P < 0.05; **P < 0.01 compared with untreated control.

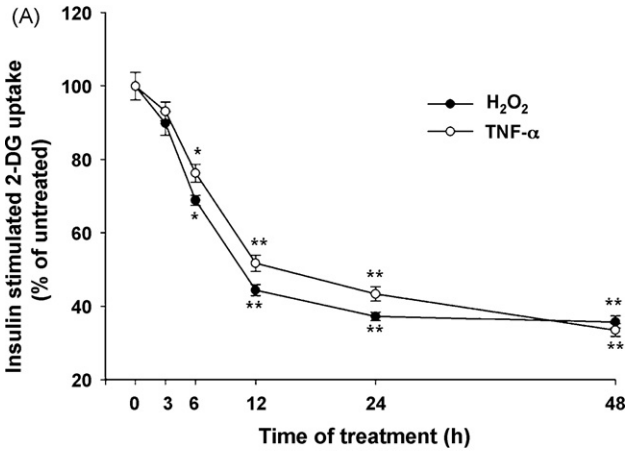

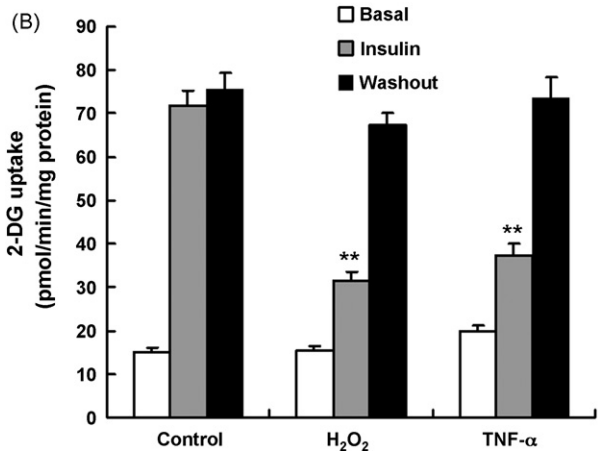

Fig. 2 – H_2O_2 and TNF-α inhibited insulin-stimulated glucose uptake in 3T3-L1 adipocytes. Serum-starved adipocytes were placed into KRP buffer without glucose, and incubated in the absence or presence of insulin (10 nM) for 30 min. Next, ^{3}H-2-DG was added for 10 min and uptake measured. (A) Adipocytes were treated with ~12 μM H_2O_2 or 1 nM TNF-α for 0–48 h, and insulin-stimulated glucose uptake was determined. (B) In washout experiments, H_2O_2 or TNF-α was removed from the medium after 12 h of incubation, and 3T3-L1 adipocytes were fed with fresh medium. Glucose uptake was assessed 12 h later in the presence of insulin. White bars, basal; gray bars, H_2O_2 or TNF-α + insulin; black bars, H_2O_2 or TNF-α washout + insulin. The data are the mean ± S.E.M. of four-independent experiments. *P < 0.05; **P < 0.01 compared with untreated control.

examined the effect of relatively low dose of H_2O_2 (~12 μM) or TNF-α (1 nM) on the insulin sensitivity in 3T3-L1 adipocytes over a 48-h time course, by assessing their abilities to uptake the glucose analogue 2-DG. As shown in the time–response curve (Fig. 2A), 6 h exposure of H_2O_2 or TNF-α to adipocytes caused a significant decrease (~30%) of insulin-stimulated glucose uptake as compared to untreated cells ($P < 0.05$). Furthermore, 12 h incubation with H_2O_2 or TNF-α led to 50–55% reduction of the insulin-dependent glucose uptake, which was similar to that seen in the clinical setting [22]. Thus, 12-h exposure was chosen as an appropriate time period and used in the following experiments. Meantime, we found that 12 h exposure of the cells to H_2O_2 or TNF-α did not affect the basal glucose transport (Fig. 2B). The H_2O_2 and TNF-α induced inhibition of insulin-stimulated glucose uptake was also recovered to control values at 12 h after washout. These observations indicate that the decreased insulin response by H_2O_2 or TNF-α was not resulted from a nonspecific toxic effect.

3.3. *Cy-3-G increased the insulin-stimulated glucose uptake in 3T3-L1 adipocytes treated with H_2O_2 or TNF-α*

As shown in Fig. 3, the insulin-stimulated glucose uptake in H_2O_2- or TNF-α-treated 3T3-L1 adipocytes was increased by pretreatment with 10–40 μM Cy-3-G in a dose-dependent manner. Meanwhile, pretreatment of the adipocytes with 1 mM NAC also attenuated the inhibition of insulin-stimulated glucose transport induced by H_2O_2, but not by TNF-α.

3.4. *Downregulation of JNK pathway and its protective effects on glucose transport and insulin signal transduction*

ROS and TNF-α are known to be potent activators of JNK whose activation is associated with insulin resistance [25]. We further examined whether JNK kinase activation mediates H_2O_2- and TNF-α-induced cellular insulin resistance using JNK1 siRNA and JNK specific inhibitor SP600125. As shown in Fig. 4A, JNK1 siRNA transfection significantly reduced the amount of intracellular JNK1 protein without affecting the control

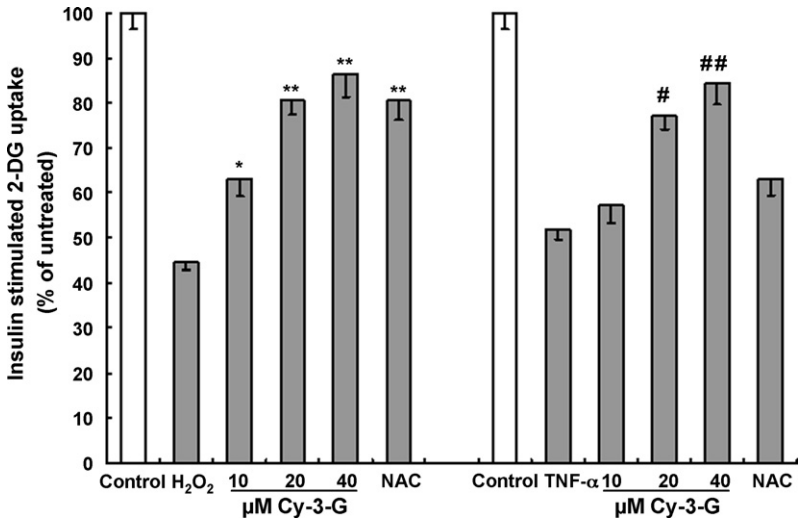

Fig. 3 – Cy-3-G improved glucose uptake capability in 3T3-L1 adipocytes treated with H_2O_2 or TNF-α. Cells were incubated for 12 h with Cy-3-G (10–40 μM) or NAC (1 mM) before exposed to ~12 μM H_2O_2 or 1 nM TNF-α. Glucose uptake was assessed 12 h later in the presence of 10 nM insulin. The data are the mean ± S.E.M. of four-independent experiments. $^{*}P < 0.05$, $^{**}P < 0.01$ compared with H_2O_2-treated control; $^{\#}P < 0.05$, $^{\#\#}P < 0.01$ compared with TNF-α-treated control.

proteins expression in 3T3-L1 adipocytes, and this silencing effect could last 48–72 h. Adipocytes transfected with JNK1 siRNA were treated with the glucose oxidase or TNF-α for 12 h, and were then subjected to the glucose transport assay. JNK1 siRNA transfection effectively prevented the inhibition of insulin-stimulated glucose uptake by treatment of H_2O_2 or TNF-α in 3T3-L1 adipocytes, compared to cells transfected with control scrambled siRNA (Fig. 4B). Moreover, 12 h pretreatment of adipocytes with 20 μM SP600125 provided a significant protection ($P < 0.05$), though not complete, against the H_2O_2 or TNF-α induced impairment in insulin-stimulated glucose transport activity (Fig. 4C).

Currently, proposed mechanism by which JNK activation leads to insulin resistance is centered on the serine 307 phosphorylation of IRS1, which is a key regulatory protein in insulin signaling [7,8]. Therefore, to identify a direct involvement of JNK activation in 3T3-L1 adipocytes insulin resistance induced by H_2O_2 or TNF-α, we measured the activation status of JNK, insulin-stimulated tyrosine phosphorylation of IRS1, and subsequent translocation of GLUT4 in SP600125 pretreated or JNK1 knockdown adipocytes. We found that JNK activation, as indicated by an increase in phosphorylated JNK band density, was stimulated by H_2O_2 and TNF-α in 3T3-L1 adipocytes after 12 h of incubation, to 2.5-fold and 2.3-fold, respectively, of untreated control (Fig. 5A and B; $P < 0.01$ each). There were no differences in the IRS1 protein expressions among control, H_2O_2- and TNF-α-treated adipocytes. However, treatment of cells with H_2O_2 or TNF-α for 12 h induced increases (182.4 ± 8.3% or 94.8 ± 5.6%) in phosphorylation of IRS1 at serine 307 as compared to control adipocytes ($P < 0.01$). In parallel, the treatments resulted in decreases (64.0 ± 2.3% or 49.5 ± 6.2%) in IRS1 tyrosine phosphorylation, and decreases (79.3 ± 3.0% or 68.5 ± 5.1%) in GLUT4 translocation, respectively (all $P < 0.01$). Pretreatment of cells with 20 μM JNK inhibitor SP600125 for 12 h resulted in a reduction of JNK activation. More importantly, blocking JNK activation by siRNA-transfection or SP600125 reversed these defects in insulin signal transduction induced by H_2O_2 or TNF-α.

3.5. *Effects of Cy-3-G on JNK activation and insulin signal transduction*

To elucidate the mechanisms mediating the protective effects of Cy-3-G on insulin sensitivity in H_2O_2- or TNF-α-treated 3T3-L1 adipocytes, we further investigated the effects of Cy-3-G on JNK activation and insulin signal transduction. As shown in Fig. 5A and B, pretreatment of Cy-3-G (over 20 μM) led to significant inhibition of JNK activation and attenuation of insulin transduction defects induced by either H_2O_2 or TNF-α (all $P < 0.05$), without altering the expression of JNK1 and IRS1 in 3T3-L1 adipocytes. In contrast, pretreatment of another antioxidant, NAC, also afforded significant protection of 3T3-L1 adipocytes against elevated JNK activation and decreased IRS1 tyrosine phosphorylation and GLUT4 translocation induced only by 12-h H_2O_2, but not TNF-α exposure.

4. Discussion

Several lines of evidence have showed that anthocyanin is effective in lowering glycemia in various experimental models of diabetes [16,17,26]. However, there has been little evidence that anthocyanins themselves are directly beneficial for the improvement of insulin sensitivity. The present study has demonstrated that Cy-3-G affords a significant protection against H_2O_2- or TNF-α-induced insulin resistance in 3T3-L1 adipocytes by blocking JNK-mediated Ser^{307} phosphorylation of IRS1. To our knowledge, this firstly demonstrated the improvement of insulin sensitivity of anthocyanin with respect to JNK signal pathway in 3T3-L1 adipocytes.

Both ROS and TNF-α are potent inducers of insulin resistance [24,27], and have physiological relevance *in vivo*

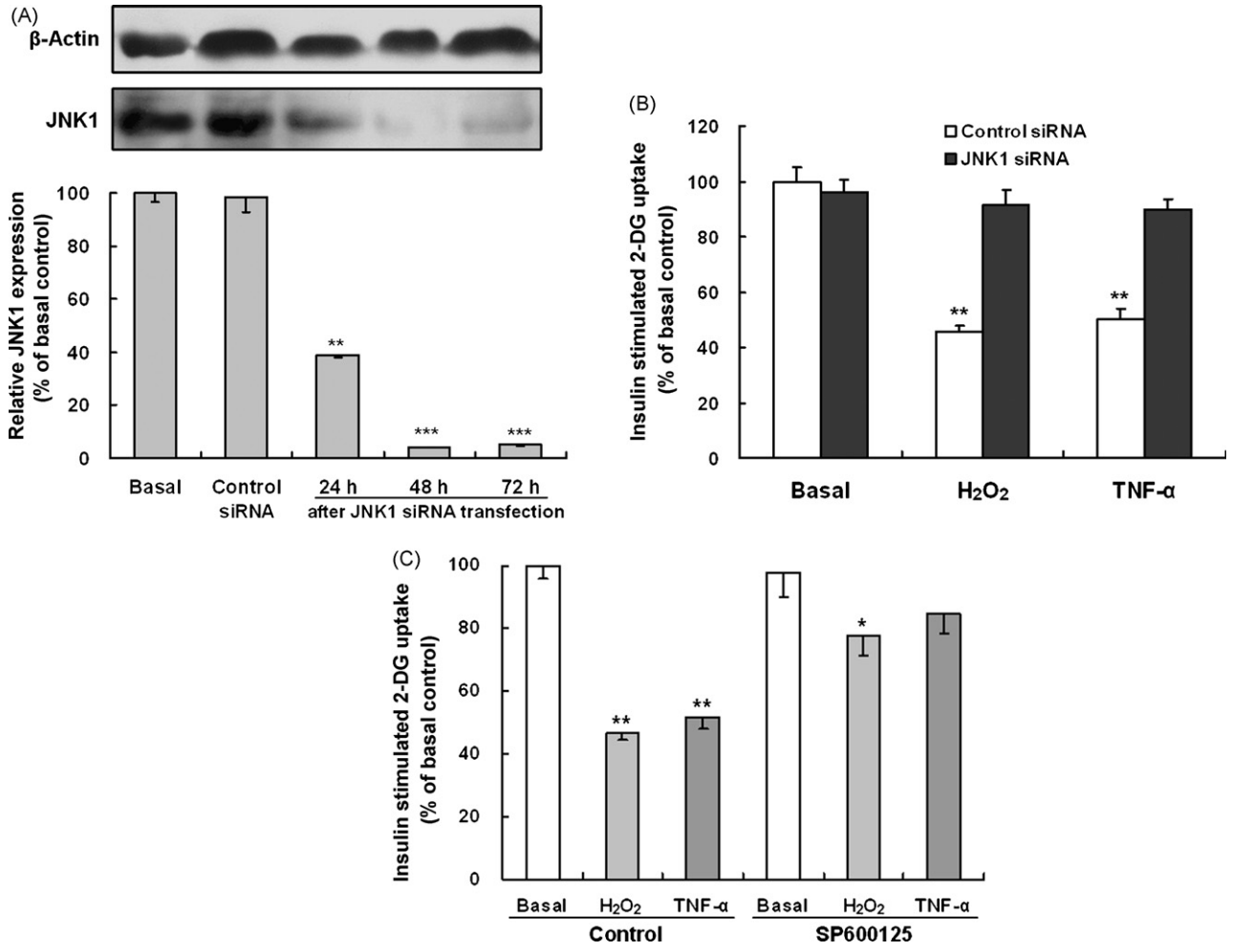

Fig. 4 – Downregulation of JNK pathway and its protective effect on insulin-stimulated glucose uptake in 3T3-L1 adipocytes treated with H_2O_2 or TNF-α. On day 6 postdifferentiation, 3T3-L1 adipocytes were transfected with JNK1 siRNA or scrambled siRNA. Twenty-four, 48 and 72 h later, cells were lysed and subjected to SDS-PAGE and Western blot analysis using JNK1 specific antibodies (A). In parallel, on day 8 postdifferentiation, siRNA-transfected (B) or SP600125 pretreated (C) adipocytes were exposed to ~12 μM H_2O_2 or 1 nM TNF-α for 12 h, and assayed for glucose uptake as above. Each bar is a mean ± S.E.M. of three-independent experiments. $^*P < 0.05$, $^{**}P < 0.01$, $^{***}P < 0.001$ compared with basal control.

[28]. Furthermore, elevated levels of ROS or TNF-α (or both) have been shown to be associated with insulin-resistant state such as steatohepatitis, obesity and metabolic syndrome [29,30]. Rudich and his colleague demonstrated that prolonged exposure of 3T3-L1 adipocytes to micromolar concentrations of H_2O_2 induces an insulin-resistant state by impairing the intracellular redox balance [20,27]. In the present study, treatment of 3T3-L1 adipocytes with TNF-α also resulted in intracellular ROS accumulation, indicating the impairments of insulin sensitivity may be related to the increased intracellular oxidative stress. A few antioxidants, including lipoic acid, vitamin E, NAC and Mn(III) tetrakis (4-benzoic acid) porphyrin (MnTBAP) have been shown to protect the cells from oxidative stress-induced insulin resistance [20,22]. Using two different cellular models of insulin resistance, we found both of Cy-3-G and NAC were capable of reducing oxidative stress induced by H_2O_2 or TNF-α. Cy-3-G ameliorated either H_2O_2 or TNF-α induced inhibition in insulin-stimulated glucose uptake in a dose-dependent manner. Differently, NAC only lowered H_2O_2, but not TNF-α-induced inhibitory effect in insulin-stimulated glucose uptake, even at higher concentration (1 mM). Thus, the insulin sensitivity improved by Cy-3-G or NAC may differ in part, and suggesting Cy-3-G induced the improvement of insulin sensitivity may be through other pathways in addition to its antioxidative action.

Despite the distinct properties between H_2O_2 and TNF-α, a possible common pathway for the inhibitory effect of H_2O_2 and TNF-α on insulin action is proposed that they may trigger a variety of serine/threonine kinase cascades [28]. However, the kinases involved are still under investigation, some molecules such as protein kinase C, inhibitor of nuclear factor κB kinase β (IKKβ), JNK, mTOR, and S6K1 are considered as candidates [8]. One attractive possibility is that H_2O_2- and TNF-α-induced insulin resistance is mediated by JNK. Recently, it has been delineated that JNK1 isoform is responsible for JNK overactivation in conditions associated with obesity and insulin resistance [31], Ablation of the *Jnk1* locus or treatment with a cell-permeable peptide inhibitor of JNK improves the

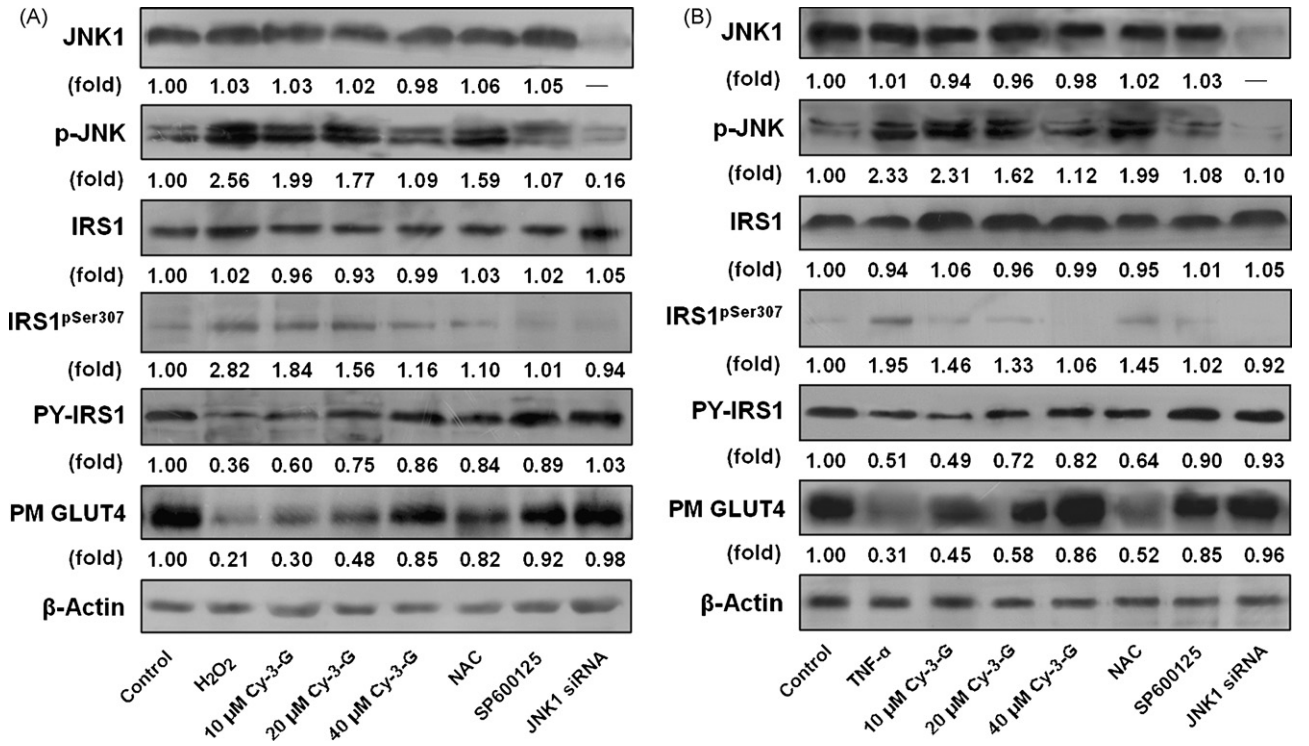

Fig. 5 – Effects of different treatments on JNK activation and insulin signal transduction. 3T3-L1 adipocytes were transfected with JNK1 siRNA or pretreated for 12 h with Cy-3-G (10–40 μM), NAC (1 mM), or SP600125 (20 μM) before exposed to H_2O_2 (A) or TNF-α (B). Cells were harvested with or without insulin stimulation, and subjected to immunoprecipitation and Western blotting analysis of JNK activation and components of the insulin signaling cascade. Representative results from three-independent experiments are shown.

insulin sensitivity in mice [9,11]. It has been proposed that ROS and TNF-α activate JNK, increase serine phosphorylation of IRS1, and decrease insulin-stimulated tyrosine phosphorylation of IRS1, leading to insulin resistance [6]. Consistent with previous reports, we found that in 3T3-L1 adipocytes, both H_2O_2 and TNF-α treatment caused significant increases in JNK activation and $IRS1^{Ser307}$ phosphorylation. Concomitantly, the insulin-stimulated IRS1 tyrosine-phosphorylation and GLUT4 translocation was markedly inhibited by H_2O_2 or TNF-α treatment. These effects were fully reversed after removing stress stimuli from the medium, demonstrating that H_2O_2 or TNF-α treatment does not produce nonspecific, toxic effects. In addition, knocking down JNK1 protein expression by its specific siRNA prevented the occurrence of insulin resistance. Our results further confirmed that the inhibitory effects of H_2O_2 and TNF-α on glucose transport and insulin signaling are largely mediated by JNK activation.

Anthocyanins are probably the most important group of visible plant pigments besides chlorophyll. Although in recent years, emerging reports have been evidenced the importance of anthocyanins as dietary antioxidants for prevention of oxidative damage, several studies gradually focused on its antidiabetic effect [17,26,32]. Cy-3-G is the widest spread anthocyanin in the plant kingdom [13]. It was reported that the *ortho*-dihydroxyphenyl structure on the B-ring of anthocyanin, which Cy-3-G also has, is essential for the health-promoting effects [33,34]. Our current data showed that the protective effect of Cy-3-G on the glucose uptake ability is similar with that of JNK-specific inhibitor SP600125 in 3T3-L1 adipocytes. Treatment of 3T3-L1 adipocytes with 40 μM Cy-3-G reversed the decreases in insulin-simulated IRS1 tyrosine phosphorylation and GLUT4 translocation to PM, and increases in JNK activation and $IRS1^{Ser307}$ phosphorylation, all of which have been considered molecular bases for H_2O_2- or TNF-α-induced insulin resistance. Overall, these results strongly suggest that Cy-3-G improved the insulin sensitivity in 3T3-L1 adipocytes exposed to H_2O_2 or TNF-α by inhibiting JNK activation.

TNF-α has been reported to increases mitochondrial ROS production and activates JNK in human hepatoma (Huh7) cells, and this observation was partially inhibited by over-expression of uncoupling protein-1 or manganese superoxide dismutase [6]. Similarly, Houstis et al. demonstrated that administration of antioxidant MnTBAP strongly reduced the level of phospho-JNK and improved the ability for insulin-stimulated glucose uptake in 3T3-L1 adipocytes [22]. As one of the possible mechanisms, scavenging ROS by Cy-3-G may contribute to the downregulation of JNK activation. In addition, TNF-α elicits a diverse array of inflammatory responses through engagement of its type-1 receptor (TNFR1). It is reported that the activation of JNK by TNF-α is initiated by coupling JNK to the TNFR1 signal transducer TNFR-associated factor-2 (TRAF2) [35]. Our previous study demonstrated that Cy-3-G interrupts CD40-induced inflammatory signaling by inhibiting TRAF2 recruitment to lipid rafts in the cellular

membrane [36]. Thus, whether Cy-3-G down-regulates JNK activation through inhibition of TRAF-2 recruitment needs further elucidated.

In conclusion, we have shown that prolonged low-grade H_2O_2 and TNF-α result in elevated JNK activation and impaired insulin-stimulated glucose transport in 3T3-L1 adipocytes. Cy-3-G effectively ameliorates H_2O_2- and TNF-α-induced insulin resistance by inhibiting the JNK-IRS1 signal pathway. These findings provide a novel insight into the therapeutic implications of anthocyanin in insulin resistance-related diseases.

Acknowledgments

This work was supported by the research grants from National Basic Research Program (973 Program, 2006CB503902) of China, and China Medical Board of New York Inc. (CMB 98-677).

REFERENCES

[1] Fletcher B, Lamendola C. Insulin resistance syndrome. J Cardiovasc Nurs 2004;19:339–45.
[2] Saltiel AR, Kahn CR. Insulin signalling and the regulation of glucose and lipid metabolism. Nature 2001;414:799–806.
[3] Johnston AM, Pirola L, Van Obberghen E. Molecular mechanisms of insulin receptor substrate protein-mediated modulation of insulin signalling. FEBS Lett 2003;546:32–6.
[4] Gao Z, Zhang X, Zuberi A, Hwang D, Quon MJ, Lefevre M, et al. Inhibition of insulin sensitivity by free fatty acids requires activation of multiple serine kinases in 3T3-L1 adipocytes. Mol Endocrinol 2004;18:2024–34.
[5] Bloch-Damti A, Potashnik R, Gual P, Le Marchand-Brustel Y, Tanti JF, Rudich A, et al. Differential effects of IRS1 phosphorylated on Ser307 or Ser632 in the induction of insulin resistance by oxidative stress. Diabetologia 2006;49:2463–73.
[6] Imoto K, Kukidome D, Nishikawa T, Matsuhisa T, Sonoda K, Fujisawa K, et al. Impact of mitochondrial reactive oxygen species and apoptosis signal-regulating kinase 1 on insulin signaling. Diabetes 2006;55:1197–204.
[7] Aguirre V, Uchida T, Yenush L, Davis R, White MF. The c-Jun NH(2)-terminal kinase promotes insulin resistance during association with insulin receptor substrate-1 and phosphorylation of Ser(307). J Biol Chem 2000;275:9047–54.
[8] Gual P, Le Marchand-Brustel Y, Tanti JF. Positive and negative regulation of insulin signaling through IRS-1 phosphorylation. Biochimie 2005;87:99–109.
[9] Hirosumi J, Tuncman G, Chang L, Gorgun CZ, Uysal KT, Maeda K, et al. A central role for JNK in obesity and insulin resistance. Nature 2002;420:333–6.
[10] Nakatani Y, Kaneto H, Kawamori D, Hatazaki M, Miyatsuka T, Matsuoka TA, et al. Modulation of the JNK pathway in liver affects insulin resistance status. J Biol Chem 2004;279:45803–9.
[11] Kaneto H, Nakatani Y, Miyatsuka T, Kawamori D, Matsuoka TA, Matsuhisa M, et al. Possible novel therapy for diabetes with cell-permeable JNK-inhibitory peptide. Nat Med 2004;10:1128–32.
[12] Clifford MN. Anthocyanins—nature, occurrence and dietary burden. J Sci Food Agric 2000;80:1063–72.
[13] Kong JM, Chia LS, Goh NK, Chia TF, Brouillard R. Analysis and biological activities of anthocyanins. Phytochemistry 2003;64:923–33.
[14] Renaud S, de Lorgeril M. Wine, alcohol, platelets, and the French paradox for coronary heart disease. Lancet 1992;339:1523–6.
[15] Alvarez Leon EE, Henriquez P, Serra-Majem L. Mediterranean diet and metabolic syndrome: a cross-sectional study in the Canary Islands. Public Health Nutr 2006;9:1089–98.
[16] Tsuda T, Horio F, Uchida K, Aoki H, Osawa T. Dietary cyanidin 3-O-beta-D-glucoside-rich purple corn color prevents obesity and ameliorates hyperglycemia in mice. J Nutr 2003;133:2125–30.
[17] Jayaprakasam B, Olson LK, Schutzki RE, Tai MH, Nair MG. Amelioration of obesity and glucose intolerance in high-fat-fed C57BL/6 mice by anthocyanins and ursolic acid in Cornelian cherry (*Cornus mas*). J Agric Food Chem 2006;54:243–8.
[18] Guo H, Ling W, Wang Q, Liu C, Hu Y, Xia M, et al. Effect of anthocyanin-rich extract from black rice (*Oryza sativa* L. indica) on hyperlipidemia and insulin resistance in fructose-fed rats. Plant Foods Hum Nutr 2007;62:1–6.
[19] Hu C, Zawistowski J, Ling W, Kitts DD. Black rice (*Oryza sativa* L. indica) pigmented fraction suppresses both reactive oxygen species and nitric oxide in chemical and biological model systems. J Agric Food Chem 2003;51:5271–7.
[20] Rudich A, Tirosh A, Potashnik R, Khamaisi M, Bashan N. Lipoic acid protects against oxidative stress induced impairment in insulin stimulation of protein kinase B and glucose transport in 3T3-L1 adipocytes. Diabetologia 1999;42:949–57.
[21] Roffey B, Atwal A, Kubow S. Cinnamon water extracts increase glucose uptake but inhibit adiponectin secretion in 3T3-L1 adipose cells. Mol Nutr Food Res 2006;50:739–45.
[22] Houstis N, Rosen ED, Lander ES. Reactive oxygen species have a causal role in multiple forms of insulin resistance. Nature 2006;440:944–8.
[23] Karlsson M, Thorn H, Parpal S, Stralfors P, Gustavsson J. Insulin induces translocation of glucose transporter GLUT4 to plasma membrane caveolae in adipocytes. FASEB J 2002;16:249–51.
[24] Stephens JM, Lee J, Pilch PF. Tumor necrosis factor-alpha-induced insulin resistance in 3T3-L1 adipocytes is accompanied by a loss of insulin receptor substrate-1 and GLUT4 expression without a loss of insulin receptor-mediated signal transduction. J Biol Chem 1997;272:971–6.
[25] Bennett BL, Satoh Y, Lewis AJ. JNK: a new therapeutic target for diabetes. Curr Opin Pharmacol 2003;3:420–5.
[26] Sasaki R, Nishimura N, Hoshino H, Isa Y, Kadowaki M, Ichi T, et al. Cyanidin 3-glucoside ameliorates hyperglycemia and insulin sensitivity due to downregulation of retinol binding protein 4 expression in diabetic mice. Biochem Pharmacol 2007;74:1619–27.
[27] Rudich A, Tirosh A, Potashnik R, Hemi R, Kanety H, Bashan N. Prolonged oxidative stress impairs insulin-induced GLUT4 translocation in 3T3-L1 adipocytes. Diabetes 1998;47:1562–9.
[28] Wellen KE, Hotamisligil GS. Inflammation, stress, and diabetes. J Clin Invest 2005;115:1111–9.
[29] Svegliati-Baroni G, Candelaresi C, Saccomanno S, Ferretti G, Bachetti T, Marzioni M, et al. A model of insulin resistance and nonalcoholic steatohepatitis in rats: role of peroxisome proliferator-activated receptor-alpha and n-3 polyunsaturated fatty acid treatment on liver injury. Am J Pathol 2006;169:846–60.
[30] Furukawa S, Fujita T, Shimabukuro M, Iwaki M, Yamada Y, Nakajima Y, et al. Increased oxidative stress in obesity and its impact on metabolic syndrome. J Clin Invest 2004;114:1752–61.

[31] Tuncman G, Hirosumi J, Solinas G, Chang L, Karin M, Hotamisligil GS. Functional *in vivo* interactions between JNK1 and JNK2 isoforms in obesity and insulin resistance. Proc Natl Acad Sci USA 2006;103:10741–6.
[32] Ghosh D, Konishi T. Anthocyanins and anthocyanin-rich extracts: role in diabetes and eye function. Asia Pac J Clin Nutr 2007;16:200–8.
[33] Hou DX, Kai K, Li JJ, Lin S, Terahara N, Wakamatsu M, et al. Anthocyanidins inhibit activator protein 1 activity and cell transformation: structure-activity relationship and molecular mechanisms. Carcinogenesis 2004;25:29–36.
[34] Hou DX, Yanagita T, Uto T, Masuzaki S, Fujii M. Anthocyanidins inhibit cyclooxygenase-2 expression in LPS-evoked macrophages: structure-activity relationship and molecular mechanisms involved. Biochem Pharmacol 2005;70:417–25.
[35] Yuasa T, Ohno S, Kehrl JH, Kyriakis JM. Tumor necrosis factor signaling to stress-activated protein kinase (SAPK)/Jun NH2-terminal kinase (JNK) and p38. Germinal center kinase couples TRAF2 to mitogen-activated protein kinase/ERK kinase kinase 1 and SAPK while receptor interacting protein associates with a mitogen-activated protein kinase kinase kinase upstream of MKK6 and p38. J Biol Chem 1998;273:22681–92.
[36] Xia M, Ling W, Zhu H, Wang Q, Ma J, Hou M, et al. Anthocyanin prevents CD40-activated proinflammatory signaling in endothelial cells by regulating cholesterol distribution. Arterioscler Thromb Vasc Biol 2007;27:519–24.